Molecular Genetics & Genomic Medicine

WILEY

Molecular Genetics & Genomic Medicine
Open Access

CLINICAL REPORT OPEN ACCESS

Homozygous Microdeletion Involving Exon 1 of *ERCC8* and *NDUFAF2* With Uniparental Isodisomy of Chromosome 5

Kaori Yamoto[1] | Kosuke Yamada[2] | Kenji Shimizu[2] | Sachiko Miyamoto[1] | Mitsuko Nakashima[1] | Hirotomo Saitsu[1]

[1]Department of Biochemistry, Hamamatsu University School of Medicine, Hamamatsu, Japan | [2]Division of Clinical Genetics and Cytogenetics, Shizuoka Children's Hospital, Shizuoka, Japan

Correspondence: Hirotomo Saitsu (hsaitsu@hama-med.ac.jp)

Received: 1 July 2024 | **Revised:** 21 October 2024 | **Accepted:** 12 November 2024

Funding: This work was supported by HUSM Grant-in-Aid Takeda Science Foundation Japan Agency for Medical Research and Development, (JP23ek0109549, JP23ek0109637, JP23ek0109674) and Japan Society for the Promotion of Science (JP20H03641, JP23H02875).

Keywords: *ERCC8* | homozygous deletion | *NDUFAF2* | RNA sequencing | uniparental disomy

ABSTRACT

Background: Uniparental isodisomy (UPiD) refers to a condition, in which both homologous chromosomes are inherited from only one parental homolog, which can result in either imprinting disorders or autosomal recessive conditions.

Methods: We performed chromosomal microarray analysis, exome sequencing (ES), and RNA sequencing (RNA-seq) using the patient's urine-derived cells on a patient with growth retardation and multiple congenital anomalies.

Results: We identified a homozygous ~0.53 kb microdeletion at 5q12.1, which was transmitted from the father with paternal UPiD(5). The deletion encompassed the first exon of both the *ERCC8* and *NDUFAF2* genes, which are responsible for Cockayne syndrome (CS) and mitochondrial complex I deficiency, respectively. Furthermore, RNA-seq confirmed the reduced expression of both genes. Indeed, in addition to clinical features common to both syndromes, such as growth retardation, developmental delay, and feeding difficulties, the patient exhibited blended phenotypes: the characteristic features of CS, including arthrogryposis, microcephaly, and facial dysmorphisms, and those of mitochondrial complex I deficiency, including high serum lactate levels and lethal apnea resulting in a severe clinical course.

Conclusion: The results imply that ES in combination with RNA-seq could be a powerful method for the detection of underlying factors responsible for rare genetic conditions, such as UPD.

1 | Introduction

Uniparental disomy (UPD) is an extremely rare condition, in which both homologous chromosomes are inherited from only one parent (Engel 1980). It is classified into two categories based on allelic status: uniparental isodisomy (UPiD) describes the inheritance of two identical chromosomes from one parent and uniparental heterodisomy (UPhD) describes the inheritance of two homologous chromosomes from one parent (Scuffins et al. 2021). Aberrant genomic imprinting caused by UPiD or UPhD can result in imprinting disorders, and furthermore, UPiD can cause rare recessive disorders due to the inheritance of pathogenic variants/deletions from heterozygous carriers (Scuffins et al. 2021). UPDs can be detected by short tandem repeat analysis or single-nucleotide polymorphism (SNP)-based microarray analysis. In recent years, with the widespread use of exome sequencing (ES), the detection rate of UPDs has increased due to various analytical methods using ES data (Scuffins et al. 2021). In addition, ES has enabled more accurate and wide-ranging identification of the region of homozygosity (ROH) and copy number variations (CNVs), as well as single-nucleotide variants, leading to faster and more accurate diagnosis.

Two neighboring genes, *ERCC8* (MIM* 609412) and *NDUFAF2* (MIM* 609653), are causative genes for Cockayne syndrome (CS) A (MIM# 216400) and mitochondrial complex I deficiency, nuclear type 10 (MC1DN10, MIM# 618233) with autosomal recessive manner, respectively. CS is caused by the loss of function of genes related to the DNA excision repair system. To date, about one hundred *ERCC8* variants, including missense and truncating variants and deletions, have been reported, accounting for approximately 30% of patients with CS (Calmels et al. 2018). CS is divided into three types according to the onset and clinical severity: type 1 (classical or moderate subtype), type 2 (early-onset or severe subtype), and type 3 (late-onset or mild subtype) (Laugel 2013). Although no clear genotype–phenotype correlation or severe form (type 2) has been reported in patients with *ERCC8* variants (Laugel 2013), a more recent study suggested that missense variants are likely to be associated with a milder phenotype than truncating variants (Calmels et al. 2018).

MC1D is caused by defects in the structural components of complex I or assembly factors that play an important role in the formation of mature protein complexes through complicated processes (Kahlhöfer, Gansen, and Zickermann 2021). *NDUFAF2* is one of the nuclear-encoded assembly factors involved in the attachment of the N module at the final stage of assembly (Kahlhöfer, Gansen, and Zickermann 2021). To date, 14 biallelic pathogenic truncating variants or deletions involving *NDUFAF2* have been described in patients with MC1DN10 (Abu Hanna et al. 2024). Furthermore, homozygous microdeletions involving both the *ERCC8* and *NDUFAF2* genes have been published in three patients (Ren et al. 2003; Janssen et al. 2009; Sabharwal et al. 2024). However, the phenotypic effects caused by the deletion of these two genes remain unclear.

Here, we report a complete UPiD of chromosome 5 [UPiD(5)] identified by chromosomal microarray analysis (CMA) in a patient with pre- and postnatal growth failure, developmental delay, arthrogryposis, dysmorphic facial features, and apnea. Further sequencing technologies, including ES and RNA sequencing (RNA-seq), revealed a homozygous microdeletion involving *ERCC8* and *NDUFAF2*, leading to a complete loss of expression of both genes. We reviewed previous literature studies regarding CS and MC1D and discussed about phenotypic heterogeneity of the patients with two gene deletions.

2 | Case Report

A Japanese female patient was found to have fetal growth restriction (FGR) and arachnoid cyst on prenatal ultrasound and was born at 38 weeks of gestation via vaginal delivery. The parents were nonconsanguineous and healthy, while her 9-year-old sister had developmental delay and several minor anomalies. At birth, the patient's length was 45.5 cm (−1.6 SD), her weight was 2386 g (−1.5 SD), and her occipitofrontal circumference (OFC) was 32.2 cm (−0.7 SD). Physical examination at 3 months of age revealed sparse scalp hair, downslanted palpebral fissures, earlobe creases, micrognathia, overhanging upper lip, bilateral single transverse palmar creases, proximal placement of bilateral halluces, proximal arthrogryposis, ectopic Mongolian spots, reticulated hyperpigmentation, and right inguinal hernia (Figure 1A). Echocardiography showed atrial septal defect, bovine aortic arch, and aberrant right subclavian artery. Slit-lamp microscopy revealed no corneal opacity, iris abnormality, or cataract although fundoscopy was not performed. She had feeding difficulties together with gastric volvulus and gastroesophageal reflux disease.

At 5 months of age, she was referred to us due to failure to thrive. Her height was 60.0 cm (−2.0 SD), her weight was 4.12 kg (−3.6 SD), and her OFC was 37.0 cm (−3.1 SD). Brain magnetic resonance imaging demonstrated an arachnoid cyst of the posterior fossa, delayed myelination of the splenium of the corpus callosum, and cerebral white matter atrophy; there were no findings of intracranial calcification, cerebellum atrophy, or symmetrical lesions in the basal ganglia or brainstem (Figure 1B). Serum lactate was persistently elevated ranging between 2.4 and 8.4 mmol/L (reference value < 2.2 mmol/L). At 6 months of age, she was admitted to the hospital due to a respiratory syncytial virus infection requiring invasive ventilation. Despite intensive care, she died from progressive pulmonary hypertension associated with mixed apnea at 8 months of age.

3 | Materials and Methods

This study was approved by the Institutional Review Board Committee at Hamamatsu University School of Medicine and Shizuoka Children's Hospital and was performed after obtaining written informed consent.

CMA, including array-based comparative genomic hybridization and SNP array, was performed using GenetiSure Dx Postnatal Assay (Agilent Technologies, Palo Alto, CA), and the obtained data were analyzed with a SureScan Dx Scanner (Agilent Technologies) by LSI Medience Corporation (Tokyo, Japan). The minimum area thresholds reported by the software were as follows: gains larger than 20 kb, losses larger than 10 kb, gains or losses containing at least 5 consecutive probes, and ROH larger than 5 Mb or containing at least 100 SNPs.

For ES, the patient's DNA was captured using the Exome 2.0 panel (Twist Bioscience, South San Francisco, CA) and sequenced on a NovaSeq6000 (Illumina, San Diego, CA) with 150-bp paired-end reads. Exome data processing, variant calling, and variant annotation were carried out, as described previously (Watanabe et al. 2021). The ROH was detected by H3M2, which is a homozygosity mapping tool using B allele frequency from ES data (Magi et al. 2014). Read-depth-based copy number variation analyses were performed using the exome-hidden Markov model (XHMM) (Fromer et al. 2012) and jNord (Nord et al. 2011; Uchiyama et al. 2021). In brief, raw CNVs detected by XHMM were filtered out when their parameters met one of the following values: Q_SOME (Phred-scaled quality of some CNV event in the interval) < 60 or segmental duplication overlapping ratios with CNVs > 90. The obtained candidate CNVs containing any coding genes were confirmed using jNord.

For RNA-seq, we obtained urine samples of the patient and cultured urine-derived cells (UDCs), as previously described (Miyamoto et al. 2023). High-quality total RNA (RINe 9.2) was used for RNA-seq and analyzed for aberrant expression levels

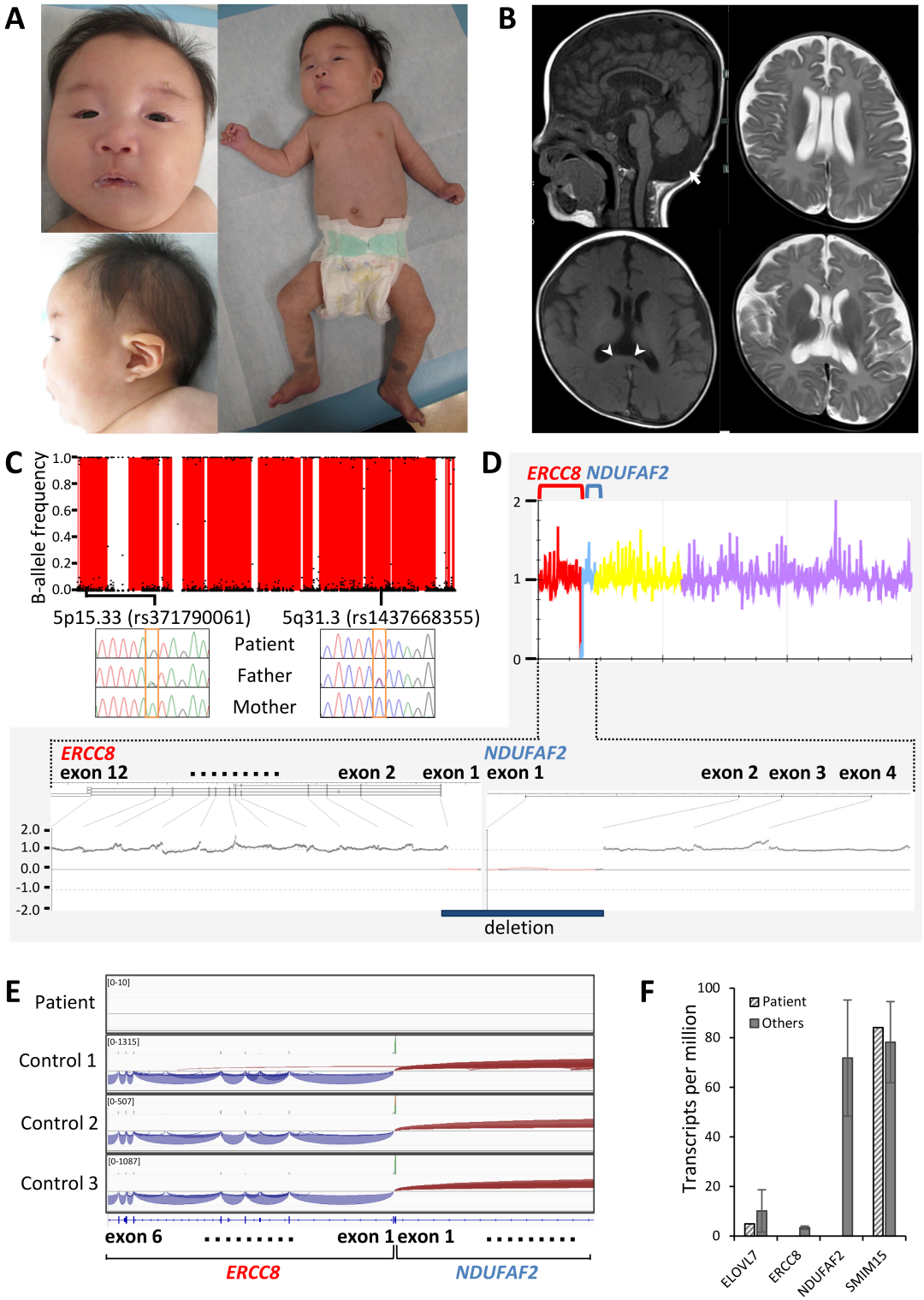

FIGURE 1 | Legend on next page.

using the detection of RNA outlier pipeline (DROP) (Kawakami et al. 2024; Yépez et al. 2021).

4 | Results

CMA showed ROH across the entire chromosome 5, indicating complete UPiD(5) (Figure S1), which was also detected by H3M2 analysis using ES data (Figure 1C). To examine the inheritance pattern of UPiD, a genotyping assay using family trio samples was performed on two SNPs on chromosome 5 (rs371790061 at 5p15.33 and rs1437668355 at 5q31.3) and identified that SNPs were homozygous in the patient, heterozygous carriers in the father, and wild-type in the mother (Figure 1C). These results suggested that the patient had complete paternal UPiD(5) [UPiD(5)pat].

FIGURE 1 | Clinical and molecular findings of the patient identified in this study. (A) Photographs of the patient at three months of age. (B) Brain magnetic resonance imaging of the patient at five months of age. The midsagittal T1-weighted image (top left) shows arachnoid cysts of the posterior fossa (arrow). The axial T2-weighted image (top right) shows ventricular dilatation and cerebral white matter atrophy. Axial T1/T2-weighted images (bottom left and right, respectively) show delayed myelination of the cerebral peduncle (arrowheads). (C) H3M2 analysis shows B allele frequency values against the genomic position, with the detection of runs of homozygosity throughout chromosome 5 (upper panel). Genotyping assay of the patient and her parents for two SNPs on 5p15.33 and 5q31.3 (highlighted with orange) indicates paternal UPiD(5) (lower panel). (D) jNord analysis reveals the homozygous deletion in *ERCC8* (red) and *NDUFAF2* (blue) genes (upper panel). In detail, the deletion (blue bar) contains exon 1 of both genes (lower panel). The *x*-axis represents the arrays of targeted genes (or exons); the *y*-axis represents log2 ratios. (E) Coverage tracks of RNA sequencing using the urinary cells from the patient, and normal controls show no aligned reads in *ERCC8* and *NDUFAF2* in the patient. (F) Number of transcripts per million for *ELOVL7*, *ERCC8*, *NDUFAF2*, and *SMIM15* genes from the RNA sequencing data of the patient (diagonal line boxes), and the other 33 samples (black boxes) demonstrate the reduced expression of both genes in the patient. The transcription levels of *ERCC8* and *NDUFAF2* are null. No significant reduction in the expression levels of *ELOVL7* and *SMIM15* is observed (*p*-values are 0.27 and 0.28, respectively).

CMA identified no pathogenic CNVs above the thresholds, except for a benign homozygous ~838 kb deletion at 5p14.1 (chr5:24,835,518-25,673,750; GRCh38/hg38) that did not contain any coding genes (Figure S1). On the other hand, XHMM with exome data detected a homozygous ~0.53 kb microdeletion at 5q12.1, encompassing *ERCC8* and *NDUFAF2* (chr5:60,944,892-60,945,422; GRCh38/hg38) (Figure S2). Moreover, jNord revealed that the deletion contained exon 1 of both genes, which are located head-to-head next to each other (Figure 1D). Quantitative real-time PCR analysis confirmed that the deletions were nullizygous in the patient and heterozygous in the father, consistent with UPiD(5)pat (Figure S3). No pathogenic or likely pathogenic variants were identified in the known genes involved in the phenotype of this patient by the single ES.

RNA-seq of patient's UDCs showed no reads mapped to all the exons of *ERCC8* and *NDUFAF2* (Figure 1E). Transcripts per million (TPM) of *ERCC8* and *NDUFAF2*, together with their nearby genes *ELOVL7* and *SMIM15*, demonstrated the reduced expression of *ERCC8* and *NDUFAF2* in the patient compared to the other 33 samples (Figure 1F). In fact, DROP software detected the expression of *ERCC8* and *NDUFAF2* in the patient as outliers.

5 | Discussion

Fifteen patients with UPiD(5) have been reported to date, all of whom developed variable autosomal recessive disorders caused by homozygosity for a single nucleoid variant carried by one parent, and there have been no reports of imprinted genes on chromosome 5 being associated with disease (Park et al. 2019; Scuffins et al. 2021). In this study, we identified the first homozygous deletion with UPiD(5). As *NDUFAF2* is located 134 bp downstream of *ERCC8* in a head-to-head orientation, the deletion encompassing the 5′ end of both genes also contained non-overlapping bidirectional promoters, resulting in a complete loss of expression of both genes.

Our patient exhibited characteristic findings of both CSA and MC1DN10 (Table 1). Some of the clinical manifestations, such as congenital microcephaly, arthrogryposis, and overhanging upper lip, were consistent with the cardinal features of the cerebro-oculo-facio-skeletal syndrome (Laugel et al. 2008), which is the most severe form of CS and partially overlaps with CS Type 2 (Laugel 2013). Meanwhile, MC1D is also characterized by FGR, growth retardation, and developmental delay. Patients with MC1D exhibit a severe clinical course and typically die from respiratory problems at a median age of 21 months. She showed an elevation of lactate level in the serum or cerebrospinal fluid, which is one of the characteristic findings of MC1D, and died of respiratory dysfunction at 8 months of age. The cardiovascular abnormalities observed in our patient, such as atrial septal defect, were not typical findings in either CSA or MC1D, since echocardiography performed on 38 patients with CS showed cardiac failure in only one case (Wilson et al. 2016). Furthermore, some characteristic features, cutaneous photosensitivity found in approximately 75% of the CS cases (Laugel 2013) and ophthalmologic abnormalities, were not observed in our patient.

Patients with CS or MC1D frequently showed brain structural abnormalities, including demyelination, basal ganglia calcification, bilateral necrotic lesions in the basal ganglia, and/or brainstem (Table 1) (Chikhaoui et al. 2022; Abu Hanna et al. 2024). However, a brain MRI at five months of age in this patient only showed cerebral white matter atrophy and delayed myelination. In this regard, it should be noted that some MC1D patients who have undergone multiple brain MRI studies have been reported to show no abnormalities on imaging despite clinical neurological findings at 6–12 months of age and subsequently demonstrate typical features of Leigh syndrome several years later (Abu Hanna et al. 2024).

We compared the clinical features of our case with those of two previously reported patients with microdeletions involving both *ERCC8* and *NDUFAF2* (Janssen et al. 2009; Sabharwal et al. 2024) and patients with variants in either *ERCC8* or *NDUFAF2* (Table 1). Janssen et al. (2009) have reported the first patient with homozygous deletion of *ELOVL7*, *ERCC8*, and *NDUFAF2*, who exhibited CS features accompanied by dysmorphic facial features, microcephaly, and DNA excision repair defect, combined with mitochondrial encephalomyopathy. The second patient with a homozygous deletion of exons 1–11 of *ERCC8* and exon 1 of *NDUFAF2* reported by Sabharwal et al. (2024) presented features of mitochondrial complex I deficiency, including dystonia, elevated cerebrospinal fluid lactate level, and midbrain hyperintensity characteristic of Leigh syndrome, without any typical features of CS. In conjunction with the fact that our patient exhibited several CS-like features but was not accompanied by any findings of encephalopathy, these findings suggested that a wide range of phenotypic heterogeneity might be observed in this contiguous gene deletion syndrome.

TABLE 1 | Clinical features of our patient and previously reported patients with microdeletion involving *ERCC8* and *NDUFAF2*, Cockayne syndrome, and mitochondrial complex I deficiency.

	Patients with the deletion involving *ERCC8* and *NDUFAF2*			Cockayne syndrome	Mitochondrial complex I deficiency
Reference	**This case**	**Janssen et al. (2009)**	**Sabharwal et al. (2024)**	**Calmels et al. (2018)**	**Abu Hanna et al. (2024)**
Variants	*ERCC8* ex 1 and *NDUFAF2* ex 1 deletion	*ELOVL7*, *ERCC8*, and *NDUFAF2* deletion	*ERCC8* ex 1–11 and *NDUFAF2* ex 1 deletion[a]	*ERCC8* variants ($n=39$)	*NDUFAF2* variants ($n=13$)[b]
Consanguinity	−	+	−	NA	7/9 (78%)
Gender	Female	Female	Female	7 females; 32 males	6 females; 4 males
Age at presentation	5 months	Birth	9 months	Birth—13 years	5 days—20 months
Age at death (median)	7 months	14 months	14 months	6–32 years ($n=5$) (13 years)	11 months—13 years ($n=9$) (21 months)
Growth					
FGR	+	+	NA	7/25 (28%)	4/4 (100%)
Microcephaly	+	+	+	26/27 (96%)	NA
Growth retardation	+	+	+	28/29 (97%)	6/7 (86%)
Developmental delay/ mental retardation	+	+	+	27/27 (100%)	8/9 (89%)
Neurological					
Arthrogryposis	+	NA	−	3/13 (23%)	NA
Myoclonus	−	−	+	NA	NA
Dystonia	−	−	+	NA	NA
Elevated serum lactate level	+	+	NA	−	4/7 (57%)
Elevated CSF lactate level	NA	NA	+	−	3/5 (60%)
Complex I activity	NA	45%	NA	−	12%–45% ($n=7$)
Cardiovascular/pulmonary					
Cardiac abnormalities	+	NA	−	NA	NA
Apnea	+	NA	NA	NA	10/10 (100%)
Gastrointestinal/hepatic					

(Continues)

TABLE 1 | (Continued)

	Patients with the deletion involving *ERCC8* and *NDUFAF2*			Cockayne syndrome	Mitochondrial complex I deficiency
Reference	**This case**	**Janssen et al. (2009)**	**Sabharwal et al. (2024)**	**Calmels et al. (2018)**	**Abu Hanna et al. (2024)**
Feeding difficulties	+	NA	NA	NA	NA
Gastroesophageal reflux disease	+	NA	NA	NA	NA
Gastrostomy	−	NA	NA	NA	4/8 (50%)
Abnormal liver function	−	NA	−	NA	NA
Ocular/auditory					
Optic atrophy	−	−	NA	NA	6/7 (86%)
Nystagmus	−	−	NA	NA	8/8 (100%)
Strabismus	−	−	NA	NA	5/5 (100%)
Cataract	−	−	NA	12/22 (54%)	NA
Retinal degeneration	−	−	NA	10/18 (55%)	NA
Hearing loss	−	NA	NA	15/21 (71%)	NA
Others					
Dysmorphic facial features	+	+	−	26/27 (96%)	NA
Dental anomalies	−	NA	NA	11/14 (78%)	NA
Photosensitivity	−	NA	−	17/23 (74%)	NA
Brain MRI					
Calcification	−	NA	−	7/7 (100%)[c]	NA
Hypomyelination	+	NA	−	4/7 (57%)[c]	NA
Cerebral white matter atrophy	+	NA	−	NA	NA
Brainstem atrophy	−	NA	−	1/7 (14%)[c]	NA
Corpus callosum hypoplasia	−	NA	−	NA	1/8 (13%)
Cerebellum atrophy	−	NA	−	4/7 (57%)[c]	1/8 (13%)

(Continues)

TABLE 1 | (Continued)

Reference	Patients with the deletion involving *ERCC8* and *NDUFAF2*			Cockayne syndrome	Mitochondrial complex I deficiency
	This case	Janssen et al. (2009)	Sabharwal et al. (2024)	Calmels et al. (2018)	Abu Hanna et al. (2024)
Abnormal signal basal ganglia	−	NA	−	NA	2/8 (25%)
Abnormal signal brainstem	−	NA	+	NA	7/8 (88%)
Abnormal signal cerebellum	−	NA	−	NA	4/8 (50%)

Abbreviations: CSF, cerebrospinal fluid; ex, exon; FGR, fetal growth restriction; NA, not available.
[a]Overlapping region of deletion of maternal and paternal alleles.
[b]The patient with *ELOVL7*, *ERCC8*, and *NDUFAF2* deletion reported by Janssen et al. is excluded.
[c]Data derived from Chikhaoui et al. (2022).

As the complete loss of expression of both genes was confirmed by RNA-seq, it is suggested that this phenotypic heterogeneity was influenced by other factors. Previous study indicated that *ERCC6*, another causative gene of CS, might complement the function of *ERCC8* (Janssen et al. 2009), while immunoblotting using fetal fibroblasts from the patient with complete loss of ERCC8 showed the downregulation of the ERCC6 protein (Sabharwal et al. 2024). In this study, RNA-seq data demonstrated no changes of *ERCC6* expression in our patient compared to controls (TPM 5.68 and 6.8 in the patient and the other 33 samples, respectively, and Figure S4) and hence showed no evidence of complementary function by the *ERCC6* gene. These results would explain the complex blended phenotype of CS and MC1D observed in this patient.

In summary, we report the first case of a homozygous deletion caused by UPiD(5). The combination of ES and RNA-seq enabled the identification of the causative gene deletion in the patient with a wide range of clinical symptoms.

Author Contributions

All authors made individual contributions to authorship. Kaori Yamoto and Sachiko Miyamoto performed molecular studies. Kosuke Yamada and Kenji Shimizu obtained clinical data and blood and urine samples. Kaori Yamoto, Mitsuko Nakashima, and Hirotomo Saitsu designed the study and wrote the manuscript. All authors reviewed and approved the final draft.

Acknowledgments

We appreciate the patient's family members for permission to publish this report. We acknowledge the NGS core facility at the Research Institute for Microbial Diseases of Osaka University for the WES sequencing. This work was supported in part by the Japan Society for the Promotion of Science, KAKENHI (Grant numbers JP20H03641 and 23H02875 (H.S.)), the Japan Agency for Medical Research and Development (AMED) (JP23ek0109549, 23ek0109674, and 23ek0109637), Takeda Science Foundation, and HUSM Grant-in-Aid from Hamamatsu University School of Medicine.

Consent

The parents of this patient have provided consent to their involvement in this report.

Conflicts of Interest

The authors declare no conflicts of interest.

Data Availability Statement

The study data that support our findings will be made available to qualified investigators upon reasonable request.

References

Abu Hanna, F., Y. Zehavi, E. Cohen-Barak, et al. 2024. "Lack of Mitochondrial Complex I Assembly Factor NDUFAF2 Results in a Distinctive Infantile-Onset Brainstem Neurodegenerative Disease With Early Lethality." *Orphanet Journal of Rare Diseases* 19, no. 1: 92.

Calmels, N., E. Botta, N. Jia, et al. 2018. "Functional and Clinical Relevance of Novel Mutations in a Large Cohort of Patients With Cockayne Syndrome." *Journal of Medical Genetics* 55, no. 5: 329–343.

Chikhaoui, A., I. Kraoua, N. Calmels, et al. 2022. "Heterogeneous Clinical Features in Cockayne Syndrome Patients and Siblings Carrying the Same CSA Mutations." *Orphanet Journal of Rare Diseases* 17, no. 1: 121.

Engel, E. 1980. "A New Genetic Concept: Uniparental Disomy and Its Potential Effect, Isodisomy." *American Journal of Medical Genetics* 6, no. 2: 137–143.

Fromer, M., J. L. Moran, K. Chambert, et al. 2012. "Discovery and Statistical Genotyping of Copy-Number Variation From Whole-Exome Sequencing Depth." *American Journal of Human Genetics* 91, no. 4: 597–607.

Janssen, R. J. R. J., F. Distelmaier, R. Smeets, et al. 2009. "Contiguous Gene Deletion of ELOVL7, ERCC8 and NDUFAF2 in a Patient With a Fatal Multisystem Disorder." *Human Molecular Genetics* 18, no. 18: 3365–3374.

Kahlhöfer, F., M. Gansen, and V. Zickermann. 2021. "Accessory Subunits of the Matrix Arm of Mitochondrial Complex I With a Focus on Subunit NDUFS4 and Its Role in Complex I Function and Assembly." *Life* 11, no. 5: 455. https://doi.org/10.3390/life11050455.

Kawakami, R., T. Hiraide, K. Watanabe, et al. 2024. "RNA sequencing and target long-read sequencing reveal an intronic transposon insertion causing aberrant splicing." *Journal of Human Genetics* 69, no. 2: 91–99. https://doi.org/10.1038/s10038-023-01211-8.

Laugel, V. 2013. "Cockayne Syndrome: The Expanding Clinical and Mutational Spectrum." *Mechanisms of Ageing and Development* 134, no. 5–6: 161–170.

Laugel, V., C. Dalloz, E. S. Tobias, et al. 2008. "Cerebro-Oculo-Facio-Skeletal Syndrome: Three Additional Cases With CSB Mutations, New Diagnostic Criteria and an Approach to Investigation." *Journal of Medical Genetics* 45, no. 9: 564–571.

Magi, A., L. Tattini, F. Palombo, et al. 2014. "H3M2: Detection of Runs of Homozygosity From Whole-Exome Sequencing Data." *Bioinformatics* 30, no. 20: 2852–2859.

Miyamoto, S., K. Nakamura, M. Kato, M. Nakashima, and H. Saitsu. 2023. "Identification of Pathogenic Deep Intronic Variant and Exonic LINE-1 Insertion in a Patient With Meckel Syndrome." *Annals of Human Genetics* 87, no. 4: 196–202.

Nord, A. S., M. Lee, M.-C. King, and T. Walsh. 2011. "Accurate and Exact CNV Identification From Targeted High-Throughput Sequence Data." *BioMed Central Genomics* 12: 184.

Park, G.-Y., D.-H. Jang, D.-W. Lee, J.-H. Jang, and J. Joo. 2019. "Hereditary Sensory and Autonomic Neuropathy 2B Caused by a Novel RETREG1 Mutation (c.765dupT) and Paternal Uniparental Isodisomy of Chromosome 5." *Frontiers in Genetics* 10: 1085.

Ren, Y., M. Saijo, Y. Nakatsu, H. Nakai, M. Yamaizumi, and K. Tanaka. 2003. "Three Novel Mutations Responsible for Cockayne Syndrome Group A." *Genes & Genetic Systems* 78, no. 1: 93–102.

Sabharwal, A., V. Gupta, S. Kv, et al. 2024. "Whole Genome Sequencing Followed by Functional Analysis of Genomic Deletion Encompassing ERCC8 and NDUFAF2 Genes in a Non-Consanguineous Indian Family Reveals Dysfunctional Mitochondrial Bioenergetics Leading to Infant Mortality." *Mitochondrion* 75: 101844.

Scuffins, J., J. Keller-Ramey, L. Dyer, et al. 2021. "Uniparental Disomy in a Population of 32,067 Clinical Exome Trios." *Genetics in Medicine: Official Journal of the American College of Medical Genetics* 23, no. 6: 1101–1107.

Uchiyama, Y., D. Yamaguchi, K. Iwama, et al. 2021. "Efficient Detection of Copy-Number Variations Using Exome Data: Batch- and Sex-Based Analyses." *Human Mutation* 42, no. 1: 50–65.

Watanabe, K., M. Nakashima, S. Kumada, et al. 2021. "Identification of Two Novel de Novo TUBB Variants in Cases With Brain Malformations: Case Reports and Literature Review." *Journal of Human Genetics* 66, no. 12: 1193–1197.

Wilson, B. T., Z. Stark, R. E. Sutton, et al. 2016. "The Cockayne Syndrome Natural History (CoSyNH) Study: Clinical Findings in 102 Individuals and Recommendations for Care." *Genetics in Medicine: Official Journal of the American College of Medical Genetics* 18, no. 5: 483–493.

Yépez, V. A., C. Mertes, M. F. Müller, et al. 2021. "Detection of Aberrant Gene Expression Events in RNA Sequencing Data." *Nature Protocols* 16, no. 2: 1276–1296.

Supporting Information

Additional supporting information can be found online in the Supporting Information section.